ACS APPLIED MATERIALS & INTERFACES

Research Article

www.acsami.org

Synthesis of Cu_2ZnSnS_4 Thin Films by a Precursor Solution Paste for Thin Film Solar Cell Applications

Jin Woo Cho,[†,‡] Agus Ismail,[†,§] Se Jin Park,[†] Woong Kim,[‡] Sungho Yoon,[⊥] and Byoung Koun Min*[,†,§,#]

[†]Clean Energy Research Center, Korea Institute of Science and Technology, 39-1 Hawolgok-dong, Seongbuk-gu, Seoul 136-791, Republic of Korea

[‡]Department of Material Sciences and Engineering and [#]Green School, Korea University, Anam-dong, Seongbuk-gu, Seoul 136-713, Republic of Korea

[§]University of Science and Technology, 176 Gajung-dong, 217 Gajungro Yuseong-gu, Daejeon 305-333, Republic of Korea

[⊥]Department of Bio & Nano Chemistry, College of Natural Sciences, Kookmin University, 861-1 Jeongneung-dong, Seongbuk-gu, Seoul 136-702, Republic of Korea

Supporting Information

ABSTRACT: Cu_2ZnSnS_4 (CZTS) is a very promising semiconductor material when used for the absorber layer of thin film solar cells because it consists of only abundant and inexpensive elements. In addition, a low-cost solution process is applicable to the preparation of CZTS absorber films, which reduces the cost when this film is used for the production of thin film solar cells. To fabricate solution-processed CZTS thin film using an easily scalable and relatively safe method, we suggest a precursor solution paste coating method with a two-step heating process (oxidation and sulfurization). The synthesized CZTS film was observed to be composed of grains of a size of ~300 nm, showing an overall densely packed morphology with some pores and voids. A solar cell device with this film as an absorber layer showed the highest efficiency of 3.02% with an open circuit voltage of 556 mV, a short current density of 13.5 mA/cm^2, and a fill factor of 40.3%. We also noted the existence of Cd moieties and an inhomogeneous Zn distribution in the CZTS film, which may have been triggered by the presence of pores and voids in the CZTS film.

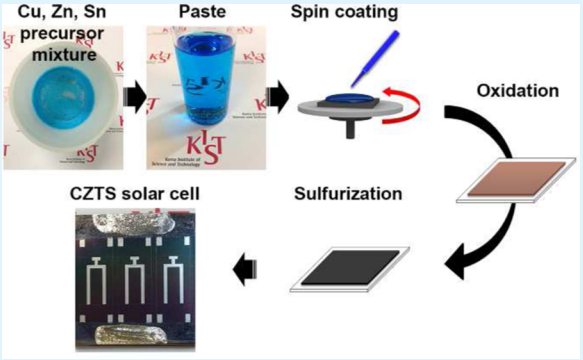

KEYWORDS: *Cu_2ZnSnS_4, CZTS, solution process, paste coating, solar cells*

INTRODUCTION

Copper-zinc-tin-sulfide (Cu_2ZnSnS_4, CZTS) film is the most important component in CZTS thin film solar cells, which have attracted substantial attention in recent years because of their beneficial properties for highly efficient and low-cost solar cells. These advantages include a large absorption coefficient (>1 × 10^4 cm^{-1}) and constituents of earth-abundant and nontoxic elements. More importantly, except for the absorber layer, the CZTS solar cell device resembles $CuInGaSe_2$ (CIGS) solar cells, which have already been commercialized, leading to the possibility of the rapid development of CZTS solar cell techniques.[1,2]

Similar to CIGS, CZTS films can be fabricated by both vacuum and solution processes. To fabricate thin film solar cells more cost-effectively, a solution process is desirable. Interestingly, in contrast to CIGS solar cells, solar cell devices created by a solution process show higher efficiency (highest efficiency of 11.1%) compared to those created by a vacuum process (highest efficiency of 9.15%).[3] The best CZTS solar cell created by a solution process was achieved by Todorov et al. using a hydrazine-based hybrid slurry approach.[4−7] However, the hydrazine that was used as solvent in their method is known to be highly toxic and explosive; therefore, it requires very restricted conditions and much caution during the film preparation process, which may limit large-scale solar cell fabrication. An air-stable and nontoxic solvent-based solution process for CZTS film preparation was reported by Woo et al. It showed the highest solar cell efficiency of 5.14%.[8] In their method, a powder mixture of Cu_2S, Zn, Sn, and S dispersed in ethanol was initially ground into nanosized particles and coated onto substrates, with a subsequent high-temperature heat treatment (530 °C) under a dilute H_2S environment.

In this study, we introduce a solution-based means of preparing CZTS thin film that involves an easily scalable, air-stable, and nontoxic solvent-based process. Instead of using micro- or nanosized precursor particles, we used metal salts that are easily soluble in ethanol. In addition, we applied an air-annealing step after coating with the precursor solution paste to

Received: January 16, 2013
Accepted: April 24, 2013
Published: April 24, 2013

   dx.doi.org/10.1021/am401210w | ACS Appl. Mater. Interfaces 2013, 5, 4162−4165

remove any residual carbon impurities which result from the use of the organic solvent and the polymer binder material. Because of the introduction of the air-annealing process we were able to decrease carbon impurity contents up to 3 at % in the CZTS film. A second heat treatment under a dilute H_2S gas environment results in the formation CZTS alloy film. A solar cell device with this film was also fabricated according to a typical CZTS solar cell configuration. With a focused ion beam (FIB) method, we also investigated the composition distribution in the CZTS film and the relationship between void formation and Cd diffusion from the CdS buffer layer.

EXPERIMENTAL SECTION

Materials. Copper nitrate hydrate ($Cu(NO_3)_2{\cdot}xH_2O$), zinc nitrate ($Zn(NO_3)_2{\cdot}xH_2O$), tin chloride dihydrate($SnCl_2{\cdot}2H_2O$), terpineol, and ethyl cellulose were all purchased from Sigma-Aldrich.

Preparation of the CZTS Thin Film. A mixture of 5.4 mmol of copper nitrate hydrate, 2.7 mmol of zinc nitrate hydrate, and 2.7 mmol of tin chloride dihydrate was formulated, which was initially mixed in a Teflon bottle using a paste mixer (PDM-300, Dae-Wha TECH) followed by the immediate removal of HCl fume by opening the bottle in a fume hood. A precursor mixture solution was then prepared by dissolving the precursor mixture in 30 mL of anhydrous ethanol followed by the addition of 20 mL of ethanol solution with 90 mmol of terpineol and 0.75 g of ethyl cellulose. After evaporating the ethanol with a rotary evaporator at 40 °C under a reduced pressure for 1 h, a viscous paste suitable for spin-coating was prepared. The paste was spin-casted at 4000 rpm for 50 s onto Mo-coated soda-lime glass substrates. The film was dried at 150 °C for 5 min in air using a hot plate. The spin-coating and drying processes were repeated two times to obtain the desired thickness. The films were then annealed in an air atmosphere at 350 °C for 1 h. Finally, a sulfurization process was conducted at 550 °C for 30 min under a $H_2S(1\%)/N_2$ gas environment.

Solar Cell Device Fabrication. A solar cell device was fabricated according to the conventional Mo/CZTS/CdS/i-ZnO/n-ZnO/Ni/Al structure. A 60 nm-thick CdS buffer layer was prepared on CZTS film by chemical bath deposition (CBD), and i-ZnO (50 nm)/Al-doped n-ZnO (500 nm) were deposited by a radio frequency magnetron sputtering method. A Ni (50 nm) and Al (500 nm) grid was prepared as a current collector by e-beam evaporation. The active area of the completed cell was 0.44 cm^2.

Characterizations. Structural characterization of the films was carried out by means of transmission electron microscopy (TEM, FEI inc., Tecnai G2, OR, USA) with a 200 kV acceleration voltage and an X-ray diffractometer (XRD, Shimadzu, XRD-6000, Tokyo, Japan) with Cu−Kα radiation (λ = 0.15406 nm). Composition analysis was carried out with electron probe microanalyzer(EPMA, JEOL Ltd., Tokyo, Japan) and energy-dispersive X-ray spectroscope (EDS, E2 V Tech. Inc., Elmsford, NY, USA). TEM-EDS mapping sample was prepared by a focused ion beam (FIB, FEI inc., Nova 600, Hillsboro, OR). The film image was measured with a scanning electron microscope (SEM, FEI inc., Nova-Nano 200, Hillsboro, OR) with an acceleration voltage of 10 kV. Raman spectroscopy was carried out using a Thermo Nicolet Almega XR model using an excitation laser with a wavelength of 532 nm. Device performances were characterized using a class AAA solar simulator (Wacom, Saitama, Japan) and an incident-photon conversion-efficiency (IPCE) measurement unit (Soma Optics, Tokyo, Japan).

RESULTS AND DISCUSSION

To prepare the precursor solution paste $Cu(NO_3)_2{\cdot}xH_2O$, $Zn(NO_3)_2{\cdot}xH_2O$, and $SnCl_2{\cdot}2H_2O$ were initially mixed in the absence of a solvent (ethanol) in a Teflon bottle using a paste mixer. HCl fume, which can arise from the hydrolysis reaction of $SnCl_2$ by water from the hydrates, generating basic salts such as Sn(OH)Cl, $Sn(OH)_2$, or $Sn(OH)_3^-$,[10] was removed by opening the cap of the bottle in a fume hood. It is noteworthy that only Cu nitrate, Zn nitrate, or Sn chloride turns into the liquid phase in an ambient condition, most likely due to solvation by moisture in the air in the absence of fume generation. On the other hand, the mixture of the three precursors after the removal of the fume led to the creation of a solid state, the shape of which persisted even when kept in an ambient condition. Mixes of two precursors (Cu nitrate + Zn nitrate, Cu nitrate + Sn chloride, and Zn nitrate + Sn chloride) were also tested. Only the mixture of Cu nitrate and Sn chloride was observed to generate fume concomitant with the release of heat. Although we did not clearly understand the nature of the precursor mixture at this point, based on our experimental observations we assumed that the HCl fume originated from the reaction between the Cu nitrate and the Sn chloride as incorporated by ambient moisture. To prepare the precursor solution paste, we dissolved the precursor mixture in anhydrous ethanol with a subsequent addition of an ethanol solution with terpineol and ethyl cellulose to adjust the viscosity so that it would be suitable for spin coating. Notably, the first precursor mixing step was necessary to dissolve all of precursors in ethanol because the precursors formed insoluble CuCl precipitates when they were directly dissolved together in ethanol.

Afterward, the precursor solution paste was spin-casted onto Mo-coated soda-lime glass substrates, with two successive heat treatments following under air and a dilute H_2S environment, respectively. Most carbon residues were eliminated by air-annealing at 350 °C. XRD did not reveal any apparent peaks, implying that an amorphous mixed oxide state of Cu, Zn, and Sn was formed after the air-annealing process. The morphologies were also investigated by SEM, as shown in images a and b in Figure 1. In spite of the presence of some pores, a 2 μm thick film was observed to be densely packed by the mixed oxide phases (Figure 1b).

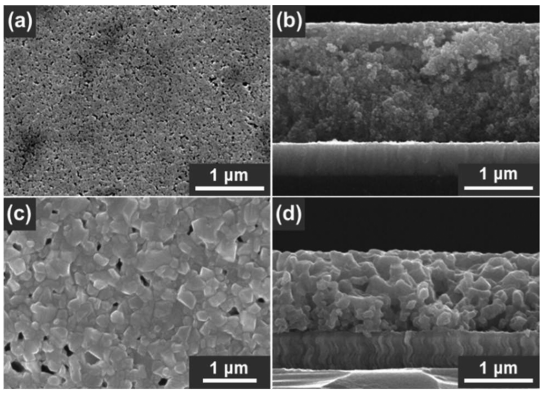

Figure 1. (a, c) Top view and (b, d) cross-sectional SEM images of the films obtained after (a, b) the air-annealing and (c, d) the sulfurization.

The second heat treatment under a $H_2S(1\%)/N_2$ gas environment resulted in significant changes in the morphology of the film (Figure 1c, d). The grains grew to a length of approximately 300 nm in concomitant with the formation of some pores on the surface because of the formation of CZTS alloy. The formation of CZTS alloy was also confirmed by the XRD pattern, as shown in Figure 2a. Specifically, the XRD pattern shows a peak at 28.4° as well as weak peaks at 47.3 and 56.1° 2θ. The most intense peak, at 28.0° 2θ, indicates the polycrystalline CZTS alloy with a (112) orientation. The other

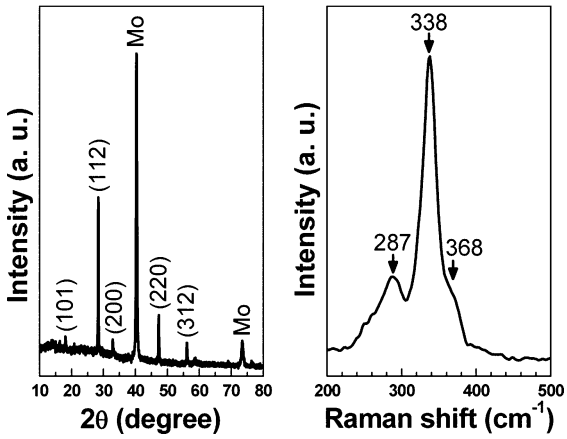

Figure 2. (a) X-ray diffraction patterns of the CZTS thin film prepared by a paste coating method. (b) Raman spectra of CZTS thin film sulfurized at 550 °C.

prominent peaks correspond to the (220) and (312) phases. In addition to these peaks commonly observed in CZTS, several weak peaks, including the (101) and (200) peaks, were also present in the XRD patterns. The presence of these peaks clearly indicates the polycrystalline kesterite structure of CZTS, which is in good agreement with the JCPDS reference (PDF #26−0575) as well as other reported values.[7,8] To further confirm the formation of kesterite film in an absence of secondary phases (e.g., ZnS and Cu_2S) Raman spectrum of the film was obtained as seen in Figure 2b. Three distinctive peaks appear at 287, 338, and 368 cm^{-1}, in agreement with well-known vibrational characteristics of kesterite CZTS film.[7−9]

The optical properties of the CZTS film were also investigated by UV−vis absorption spectroscopy. As shown in Figure 3, the film absorbs light with higher energy than 1000

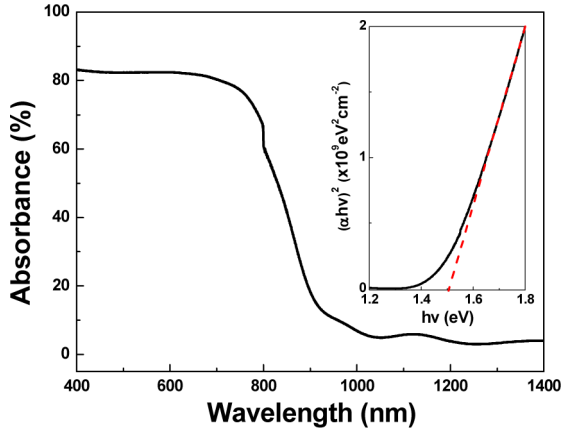

Figure 3. UV−vis spectra of the CZTS thin film prepared by a paste coating method. The inset shows a plot of $(\alpha h\nu)^2$ vs $h\nu$ to evaluate the band gap.

nm. Notably, the absorbance (%) in Figure 3 was estimated through absorbance (%) = 100% − transmittance (%) − reflectance (%) using the CZTS film separately prepared on a bare glass substrate with an identical synthetic method to that on a Mo-coated glass substrate (see Figure S1 in the Supporting Information).[11] The optical band gap was also estimated to be 1.5 ± 0.02 eV based on the plot of $(\alpha h\nu)^2$ vs $h\nu$, as shown in the inset of Figure 3.

Using the synthesized CZTS films, solar cell devices were constructed. The general substrate-type configuration (Mo/CZTS/CdS/i-ZnO/n-ZnO/Ni/Al) and formulations were applied to fabricate devices in which a CdS buffer layer and a ZnO window layer were prepared by chemical bath deposition (CBD) and sputtering deposition methods, respectively. As shown in Figure 4a, the current density−voltage (J−V)

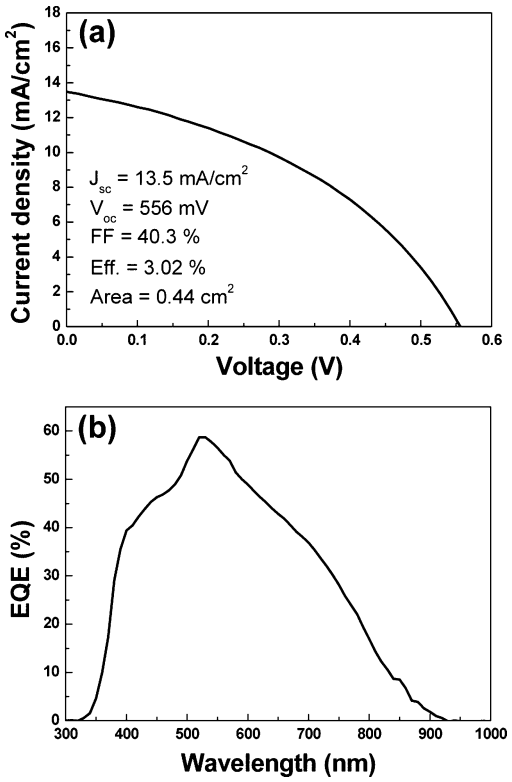

Figure 4. (a) Current density−voltage (J−V) characteristics and (b) external quantum efficiency (EQE) curve of the CZTS solar cell device.

characteristics of the devices revealed the highest efficiency of 3.02% with an open circuit voltage (V_{oc}) of 556 mV, a short circuit current density (J_{sc}) of 13.5 mA/cm^2, and a fill factor (FF) of 40.3%.

Despite these efforts, the solar cell efficiency was not sufficiently high. To gain insight into the possible reasons for the low efficiency, we investigated the compositional distribution of the CZTS film related to the presence of some pores and voids. For this investigation, the integrated film was precisely milled by a focused ion beam technique, as shown in Figure 5. The presence of large voids is clearly observable in the CZTS film. To analyze the composition of the CZTS film, a certain area of the film with voids (marked by the dotted line) was mapped by EDS, as shown in Figure 5b−f. It is clear that sulfur is homogeneously distributed in the entire area of the film except in the void region (Figure 5c). The compositions of the distributions of copper and tin were also similar, in which small amounts of Cu and Sn were found in near void regions (Figure 5d, f). Interestingly, however, Zn revealed a substantially inhomogeneous distribution in which some specific local regions (seemingly near voids) contained higher concentrations than other areas (Figure 5e). It is known that secondary phases such as Cu_3SnS_4, ZnS, and MoS_2 form during the preparation of CZTS film, which is considered to be a

dx.doi.org/10.1021/am401210w | ACS Appl. Mater. Interfaces 2013, 5, 4162−4165

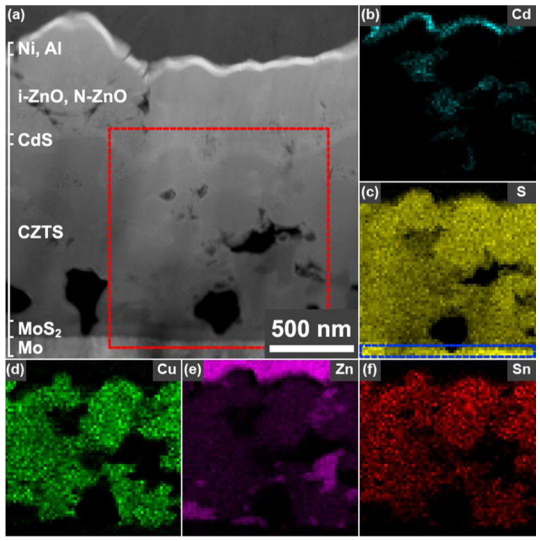

Figure 5. (a) Cross-sectional TEM image of the integrated film (CZTS/CdS/ZnO) milled by a focused ion beam technique and (b–f) the EDS mapping for the compositional distribution ((b) Cd, (c) S, (d) Cu, (e) Zn, and (f) Sn) in the certain area (marked by the dotted line in a) of the CZTS film.

serious problem when attempting to create highly efficient solar cells.[12,13] In particular, it was evident that ZnS secondary phase formed at a deep region of the film.[12] The relatively high concentration of Zn at a localized area in our film may be related to the formation of these ZnS secondary phases. In addition, we noted that a 100 nm thick MoS_x layer develops at the interface between the CZTS and the Mo as a consequence of an inter-reaction, as revealed by the brighter contrast of the S distribution (marked by the dotted line) in Figure 5c. Importantly, we also found Cd moieties in the CZTS film, as shown in Figure 5b. These CdS originated from the CdS buffer layer. This is also frequently observed in CIGS solar cells.[14−16] Furthermore, the presence of pores and voids may accelerate Cd diffusion in the CIGS film.[16] Indeed, a higher concentration of Cd was observed in the void region in our CZTS absorber layer.

CONCLUSIONS

In summary, CZTS thin films were prepared by a precursor solution paste. By applying air annealing and a subsequent sulfurization process we synthesized polycrystalline CZTS film with only a slight amount of carbon impurity. In spite of the presence of some pores and voids, the as-synthesized CZTS film showed a very densely packed morphology. A solar cell device with this film as an absorber layer showed the highest efficiency of 3.02%. We also observed the existence of Cd moieties and an inhomogeneous Zn distribution in the CZTS film by a focused ion beam technique and by EDS mapping.

ASSOCIATED CONTENT

Supporting Information

UV−vis absorption, XRD, and Raman data of the CZTS thin films. This material is available free of charge via the Internet at http://pubs.acs.org/.

AUTHOR INFORMATION

Corresponding Author

*E-mail: bkmin@kist.re.kr (B.K.M.).

Notes

The authors declare no competing financial interest.

ACKNOWLEDGMENTS

This work was supported by National Research Foundation of Korea Grant (NRF-2009-C1AAA001-0092935) and by the University-Institute cooperation program (2012) funded by the Korean Government (MEST). The authors thank the program of Korea Institute of Science and Technology (KIST).

REFERENCES

(1) Siebentritt, S.; Schorr, S. *Prog. Photovoltaics* **2012**, *20*, 512−519.
(2) Ramasamy, K.; Malik, M. A.; O'Brien, P. *Chem. Commun.* **2012**, *48*, 5703−5714.
(3) Repins, I.; Beall, C.; Vora, N.; DeHart, C.; Kuciauskas, D.; Dippo, P.; To, B.; Mann, J.; Hsu, W. C.; Goodrich, A.; Noufi, R. *Sol. Energy Mater. Sol. Cells* **2012**, *101*, 154−159.
(4) Todorov, T. K. T., J.; Bag, S.; Gunawan, O.; Gokmen, T.; Zhu, Y.; Mitzi, D. B. *Adv. Energy Mater.* **2013**, *3*, 34−38.
(5) Bag, S.; Gunawan, O.; Gokmen, T.; Zhu, Y.; Todorov, T. K.; Mitzi, D. B. *Energy Environ. Sci.* **2012**, *5*, 7060−7065.
(6) Todorov, T. K.; Reuter, K. B.; Mitzi, D. B. *Adv. Mater.* **2010**, *22*, E156−E159.
(7) Wenbing Yang, H.-S. D.; Bob, B.; Zhou, Huanping; Lei, Bao; Chung, C.-H.; Li, Sheng-Han; Hou, W. W.; Yang, Y. *Adv. Mater.* **2012**, *24*, 6323−2329.
(8) Woo, K.; Kim, Y.; Moon, J. *Energy Environ. Sci.* **2012**, *5*, 5340−5345.
(9) Wang, K.; Gunawan, O.; Todorov, T.; Shin, B.; Chey, S. J.; Bojarczuk, N. A.; Mitzi, D.; Guha, S. *Appl. Phys. Lett.* **2010**, *97*, 143508.
(10) Seby, F.; Potin-Gautier, M.; Giffaut, E.; Donard, O. F. X. *Geochim. Cosmochim. Acta* **2001**, *65*, 3041−3053.
(11) Niki, S.; Contreras, M.; Repins, I.; Powalla, M.; Kushiya, K.; Ishizuka, S.; Matsubara, K. *Prog. Photovoltaics* **2010**, *18*, 453−466.
(12) Wang, K.; Shin, B.; Reuter, K. B.; Todorov, T.; Mitzi, D. B.; Guha, S. *Appl. Phys. Lett.* **2011**, *98*, 051912.
(13) Fontane, X.; Calvo-Barrio, L.; Izquierdo-Roca, V.; Saucedo, E.; Perez-Rodriguez, A.; Morante, J. R.; Berg, D. M.; Dale, P. J.; Siebentritt, S. *Appl. Phys. Lett.* **2011**, *98*, 181905.
(14) Nakada, T. *Thin Solid Films* **2000**, *361*, 346−352.
(15) Liao, D. X.; Rockett, A. *J. Appl. Phys.* **2003**, *93*, 9380−9382.
(16) Lei, C.; Duch, M.; Robertson, I. M.; Rockett, A. *J. Appl. Phys.* **2010**, *108*, 114908.